NANO LETTERS

Letter

pubs.acs.org/NanoLett

Tip-triggered Thermal Cascade Manipulation of Magic Number Gold–Fullerene Clusters in the Scanning Tunnelling Microscope

Dogan Kaya,[†,§] Deliang Bao,[‡,∥] Richard E. Palmer,[⊥] Shixuan Du,*[,‡] and Quanmin Guo*[,†]

[†]School of Physics and Astronomy, University of Birmingham, Edgbaston, Birmingham B15 2TT, United Kingdom

[‡]Institute of Physics, Chinese Academy of Sciences, Beijing 100190, China

[§]Physics Department, Faculty of Arts and Sciences, Sakarya University, Serdivan, Sakarya 54050, Turkey

[∥]The University of Chinese Academy of Sciences, Beijing 100049, China

[⊥]College of Engineering, Swansea University, Bay Campus, Fabian Way, Swansea SA1 8EN, United Kingdom

Supporting Information

ABSTRACT: We demonstrate cascade manipulation between magic number gold–fullerene hybrid clusters by channelling thermal energy into a specific reaction pathway with a trigger from the tip of a scanning tunnelling microscope (STM). The $(C_{60})_m$–Au_n clusters, formed via self-assembly on the Au(111) surface, consist of n Au atoms and m C_{60} molecules; the three smallest stable clusters are $(C_{60})_7$–Au_{19}, $(C_{60})_{10}$–Au_{35}, and $(C_{60})_{12}$–Au_{49}. The manipulation cascade was initiated by driving the STM tip into the cluster followed by tip retraction. Temporary, partial fragmentation of the cluster was followed by reorganization. Self-selection of the correct numbers of Au atoms and C_{60} molecules led to the formation of the next magic number cluster. This cascade manipulation is efficient and facile with an extremely high selectivity. It offers a way to perform on-surface tailoring of atomic and molecular clusters by harnessing thermal energy, which is known as the principal enemy of the quest to achieve ultimate structural control with the STM.

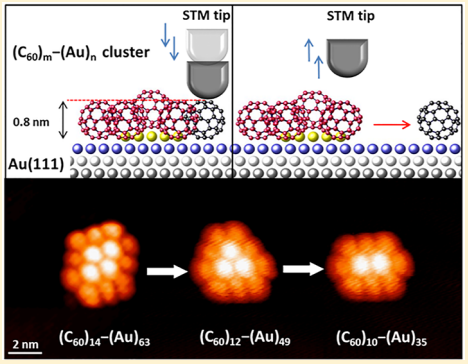

KEYWORDS: *Cluster, self-assembly, atom manipulation, nanostructures, scanning tunneling microscopy, fullerene*

Clusters and nanoparticles of selected size, whether naked or ligated, have now become an important class of materials in a number of scientifically and technologically important areas.[1−6] In most potential applications, clusters need to be deposited on a solid surface where they are electronically, optically, or chemically integrated into a device. Thus, the need for tailoring/processing of the clusters once they are on the support is obvious. Scanning probe microscopes (SPM), such as the scanning tunnelling microscope (STM) and the atomic force microscope (AFM), with the capability of manipulating materials atom-by-atom[7−13] are at least in principle powerful tools for on-surface tailoring of clusters. A major disadvantage of SPM-based techniques is that atom-by-atom manipulation is intrinsically slow and, in most cases, has to be conducted at cryogenic temperatures. However, considerable progress has been made in recent years, such that multiple events can now be driven by a single trigger from the STM,[14−20] making it a more practical manipulation tool. Nevertheless, operations performed by the STM are always in competition with thermal processes, which can make single-atom/molecule-based STM manipulations unfeasible under important conditions, most noticeably at room temperature (RT) because thermal energy tends to wipe out whatever is written by the STM. Most desirable for on-surface tailoring of clusters would be the ability to trigger an initial reaction with the STM, which provokes the cluster to reorganize using thermal energy. This way, the adverse effect of thermal energy is turned into a beneficial driver for STM-induced cluster/nanoparticle reorganization. Here, we report such a process where hybrid $(C_{60})_m$–Au_n clusters are selectively downsized from one magic number to another at RT with high efficiency and accuracy.

The magic number $(C_{60})_m$–Au_n clusters were discovered recently[21] when C_{60} molecules and Au atoms are allowed to interact on a Au(111) substrate. These clusters have a Au core in the shape of a regular two-dimensional Au island and a shell of C_{60} molecules with only certain combinations of m and n allowed. The $(C_{60})_m$–Au_n cluster is stabilized by charge transfer from Au to the molecule and van der Waals interaction among the molecules. The clusters are mostly located in the fcc region next to the elbow site, although a small number of them are found in the fcc region at some distance away from the elbows. When we use the tip of the STM to extract one or two molecules from a cluster at RT, we find that the remaining molecules and atoms are able to respond collectively by self-selecting the correct number of molecules and atoms such that

Received: July 3, 2017
Revised: August 6, 2017
Published: September 14, 2017

DOI: 10.1021/acs.nanolett.7b02802
Nano Lett. 2017, 17, 6171−6176

a new magic number cluster of one size smaller is assembled. The STM tip merely provides the initial triggering to disrupt the stable cluster, while the accurate and fast assembly process toward the formation of the new magic number cluster is completely in the hands of the atoms and molecules. The interaction of the C_{60} molecule with the Au(111) substrate has been studied rather extensively both in our laboratory[22,23] and by others,[24−27] providing a solid ground for the present investigation.

Manipulation of the cluster is conducted by driving the STM tip into a C_{60} molecule as shown schematically in Figure 1. In

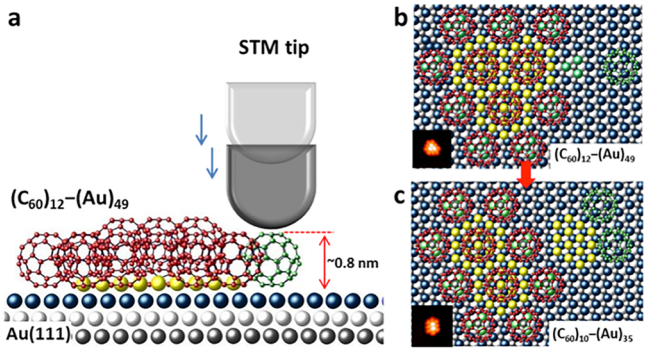

Figure 1. Schematic of the manipulation experiment. (a) The tip is located directly above a preselected molecule (green colored C_{60}) at the edge of a cluster. It then moves toward the molecule by 1.2 nm. This is sufficient to detach the molecule from the cluster. A clean W tip is illustrated in the diagram, although in reality the tip is likely to be coated with Au atoms. (b) As the tip withdraws, the displaced molecule either diffuses away or becomes attached to the tip. Green colored spheres represent first-layer Au atoms that are in direct contact with C_{60} molecules. (c) The remaining atoms and molecules within the broken cluster reorganize to form a new magic number cluster by releasing excess C_{60} molecules and Au atoms.

reality the tip is likely to be covered by Au atoms. There is also the possibility that a C_{60} molecule becomes attached to the tip. We did not study how the manipulation process is affected by the tip state. A clean W tip is drawn in the diagram for simplicity. One of the molecules (green colored C_{60}) at the edges of the Au island is targeted. The exact initial distance between the tip and the C_{60} molecule is not known, but it is controlled by fixed tunnel parameters: −1.67 V sample bias and 47 pA tunnel current. The tip moves from its initial location toward the surface by 1.2 nm and then returns to its starting position. The complete journey takes 12.8 ms. Contacting C_{60} molecules by the STM tip has been thoroughly investigated previously,[28−30] and it was demonstrated that, by following how the current changes as a function of tip−surface distance, the point of contact between the tip apex and the molecule on the surface can be accurately defined. Based on the findings of Schull et al.,[28] and the set point of −1.67 V sample bias and 47 pA tunnel current used in our experiment, we estimated that in our study the distance traveled by the STM tip before reaching contact with C_{60} is ~0.5 nm. This estimation, however, involves a large uncertainty. An independent way of obtaining the initial tip height is given in the Supporting Information. The total displacement of 1.2 nm of the tip suggests that the tip apex nearly reached the Au(111) substrate during approach. The tip is therefore physically inserted into the space between neighboring molecules. This is consistent with the observation of laterally displaced C_{60} molecules when manipulation is performed at 110 K (Figure S1, Supporting Information). Before we attempted to manipulate the $(C_{60})_m$−Au_n clusters, a large number of experiments had been conducted on extended C_{60} monolayers to find out the best condition for extracting C_{60} molecules. It is found that the vertical distance traveled by the STM tip has a strong influence on the number of molecules removed (Supporting Information). It is not possible to extract C_{60} molecules if the distance traveled by the STM tip is shorter than 1.2 nm. Two or three molecules can be extracted if the distance traveled is between 1.6 and 1.8 nm. However, with the distance traveled by the tip greater than 1.4 nm, there is evidence that the tip touches the Au(111) substrate leading to local damage. To manipulate the cluster, we move the tip by 1.2 nm, which is found to be the optimal condition for cleanly displacing a single molecule with a high (80%) success rate. This success rate is evaluated from more than 200 independent manipulation events. Once the tip returns to its initial height after the manipulation event, it scans the cluster under normal imaging conditions so that any changes brought to the cluster can be revealed by directly comparing the images before and after the manipulation event. Figure 1b,c illustrates the transformation from $(C_{60})_{12}$−Au_{49} to $(C_{60})_{10}$−Au_{35}, a process that has been successfully conducted as described in the following section.

STM images shown in Figure 2 demonstrate the cascade manipulation of $(C_{60})_m$−Au_n clusters. In Figure 2a there is a

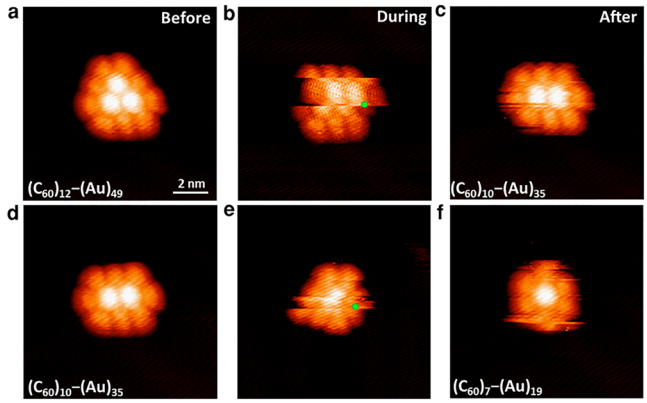

Figure 2. Tip-triggered cascade cluster transformation. (a−c) Transformation from $(C_{60})_{12}$−$(Au)_{49}$ to $(C_{60})_{10}$−$(Au)_{35}$. (d−f) Transformation from $(C_{60})_{10}$−$(Au)_{35}$ to $(C_{60})_7$−$(Au)_{19}$. Green dots in (b) and (e) indicate the locations where the tip is driven toward the C_{60} molecule.

typical $(C_{60})_{12}$−Au_{49} cluster with three molecules sitting above the Au island and nine molecules sitting around the edges of the Au island.[21] In Figure 2b, the tip scans upward and stops at the point highlighted by a green dot where the tip moves vertically down toward the molecule by 1.2 nm. It then withdraws and continues to scan to complete the whole frame. The discontinuity of the image manifested by a sudden offset of the molecules to the right-hand side after the manipulation is a clear sign of the reorganization of the cluster. Although Au atoms are covered by the molecules and hence not directly visible in the images, their movements can be identified by following the positions of the "bright" molecules. This is because there is a layer of Au atoms sandwiched between the Au(111) substrate and the bright C_{60} molecule. A second discontinuity in the image (offset to the left), Figure 2b, registers further gross movement of the molecules and the

DOI: 10.1021/acs.nanolett.7b02802
Nano Lett. 2017, 17, 6171−6176

associated Au atoms without deliberate intervention of the STM tip. As will be shown later, thermally induced cluster transformation can take place in the absence of a deliberate STM trigger, albeit with a very low probability at RT. We have noticed that once a cluster is disturbed by the STM trigger, it exhibits a higher level of activity within about 10 s before settling down. During this short window of high activity, the cluster is seen to adjust its location/shape. It is not clear though what controls this active period of time. The movement of the molecules occurs within a much shorter time scale than the time taken for a single scan line. When the tip comes back to scan the cluster again, it finds a new stable cluster shown in Figure 2c. The newly formed cluster is a $(C_{60})_{10}$–Au_{35} magic number cluster.[21] Thus, the $(C_{60})_{12}$–Au_{49} cluster has transformed into a $(C_{60})_{10}$–Au_{35} cluster by losing two C_{60} molecules and 14 Au atoms. One of the two molecules is removed by the STM tip during the initial triggering event. It is not known if Au atoms are also removed during the triggering process, and if so, how many are removed. Without the deliberate manipulation by the STM tip, the magic number clusters show rather high stability at RT. Only occasionally, once every few hours, e.g., a cluster is observed to change from one orientation to another due to pure thermal activation. No thermally induced downsizing of clusters is ever observed at RT. At high enough temperatures, >420 K, all magic number clusters become unstable and disintegrate completely without selectivity.

Further manipulation can be performed on the newly formed $(C_{60})_{10}$–Au_{35}. Figure 2d–f shows the transformation of this $(C_{60})_{10}$–Au_{35} cluster into a $(C_{60})_7$–Au_{19} cluster. The $(C_{60})_7$–Au_{19} cluster is the smallest stable hybrid cluster.[21] If a C_{60} molecule is removed from $(C_{60})_7$–Au_{19}, complete fragmentation of the cluster will take place. Transformation from $(C_{60})_{10}$–Au_{35} to $(C_{60})_7$–Au_{19} involves the removal of three C_{60} molecules and 16 Au atoms. Again, one of the three removed molecules is displaced by the tip during the triggering step. In Figure 2e, a rapid change, within the time for a single scan line occurs after the trigger is applied giving rise to a typical discontinuity of the recorded image. Upper part of the image after the discontinuity line already shows the sign of a $(C_{60})_7$–Au_{19} cluster. The full structure of the $(C_{60})_7$–Au_{19} cluster is revealed in Figure 2f. A number of STM images taken in between Figure 2e,f shows that the $(C_{60})_7$–Au_{19} cluster remains quite "active" after it is formed, and it takes a relatively long time before it settles down (Figure S4, Supporting Information). The cluster seems to have rotated with the close-packing direction of the $(C_{60})_7$–Au_{19} cluster different from that of its parents and grandparents by 30°. This cannot be fully explained with the model we proposed[21] and requires some further investigation.

Data shown in Figure 2 leads to the following conclusion. When a C_{60} molecule is removed from the edge of a magic number $(C_{60})_m$–Au_n cluster, the cluster spontaneously reorganizes to form another magic number cluster one size smaller. The formation of the smaller magic number cluster, $(C_{60})_p$–Au_q, requires an exact combination of p and q. Hence, some Au atoms and C_{60} molecules become redundant and are released. At RT, the released atoms and molecules, unable to form a stable structure of their own, diffuse away to surface steps. Although an exact combination of p and q is required to form a new stable cluster, this requirement is fulfilled by the work of the molecules and atoms. In the cascade manipulation steps shown in Figure 2, the accuracy of the STM trigger is controlled to remove one C_{60} molecule. There is no need for the STM tip to remove an accurate number of Au atoms from the starting cluster. The cluster is able to keep the correct numbers of Au atoms as well as C_{60} molecules. The STM tip is there to trigger the cluster transformation, and it seems that this trigger does not have to be error free.

Cascade manipulation of the $(C_{60})_m$–Au_n cluster as described above depends on the location of the STM trigger. If the trigger is applied to a C_{60} molecule sitting above the Au island, rather than one at the edge, the cluster remains stable after one molecule is removed, as demonstrated in Figure 3. Here we

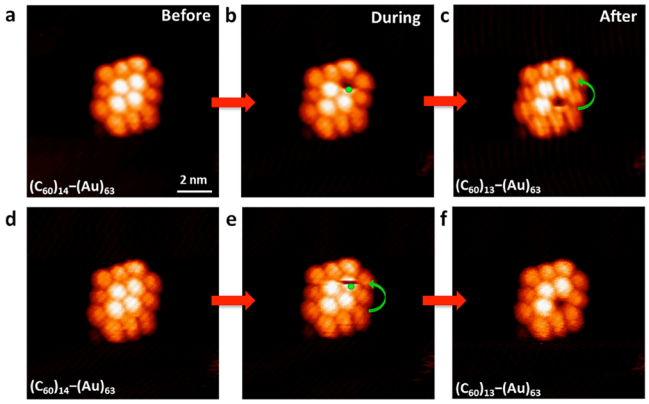

Figure 3. Single molecule extraction. (a–c) STM images showing the consequence of applying the manipulation trigger on a C_{60} molecule sitting above the Au island. The cluster here is $(C_{60})_{14}$–$(Au)_{63}$. (d–f) Similar manipulation performed on another $(C_{60})_{14}$–$(Au)_{63}$ cluster. Green dots in (b) and (e) indicate the locations where the triggers are applied. Green curved arrows indicate vacancy filling by diffusing C_{60} molecules.

have a $(C_{60})_{14}$–Au_{63} cluster in Figure 3a. Four molecules sit above a 63 Au atom island. In Figure 3b, an STM trigger is applied resulting in the removal of a C_{60} molecule. The molecules sitting at the edges of the Au island are not affected by this trigger. The Au island, under the protection of the ten molecules at the edges, keeps its integrity. Figure 3c shows that the initial vacancy created becomes filled when the C_{60} below the vacancy moves up. Figure 3d–f shows another operation on a different $(C_{60})_{14}$–Au_{63} cluster. Figure 3e clearly shows that the vacancy created by the trigger is filled within ~seconds by the molecule from below. The vacancy is mobile at RT, and it can be filled by any of the two nearest neighbor "bright" molecules (Supporting Information). Once a vacancy is created, removal of the remaining three "bright" molecules become much more difficult. The approaching STM tip causes lateral movement, rather than extraction, of the remaining molecules. This further suggests that the initial ejection of the C_{60} molecule is due to tip-induced compression, i.e., the molecule is squeezed out. The Au island seems to be stable as long as the step edges of the island are protected by the molecules. The vacancy, albeit mobile, does not diminish. This suggests no loss of Au atoms when the vacancy is created.

As mentioned before, with 1.2 nm distance of tip approach, the probability that a single C_{60} molecule is removed from the cluster is 0.8. Even when no molecule is removed from the cluster, the cluster can still change as shown in Figure 4. Here a trigger is applied to a molecule on the side of a $(C_{60})_{12}$–Au_{49} cluster. This time, no molecule is removed from the cluster. However, the cluster has undergone significant changes. Comparing the images in Figure 4a,c, the cluster seems to

DOI: 10.1021/acs.nanolett.7b02802
Nano Lett. 2017, 17, 6171–6176

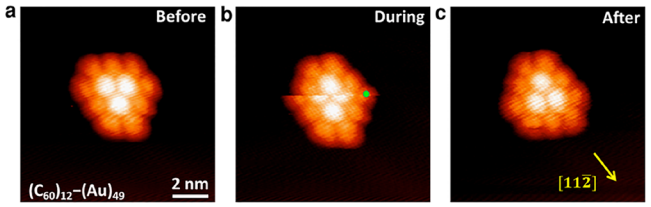

Figure 4. Tip-triggered rotation of a cluster. (a–c) STM images showing the flipping of a $(C_{60})_{12}$–$(Au)_{49}$ cluster triggered by the STM tip. Green dot in (b) indicates where the trigger is applied. The molecule targeted by the tip has not been removed. The cluster collectively changes its orientation.

have flipped upside down. This "flipping" occurs immediately after the triggering event as shown in Figure 4b. It happens at a much faster time scale than what the STM can follow.

The $(C_{60})_{12}$–Au_{49} cluster has retained its integrity following the STM trigger. The flipping of the cluster indicates a significant level of mass movement within the cluster. Obviously, the cluster is unable to stand up collectively and flip. It is more likely that the initial trigger has momentarily disrupted the cluster. A complete reorganization of molecules and atoms then takes place. The clusters in Figure 4a,c are two equivalent configurations. Sometimes we observe cluster rotation at RT without the intervention of the STM. Figure 5

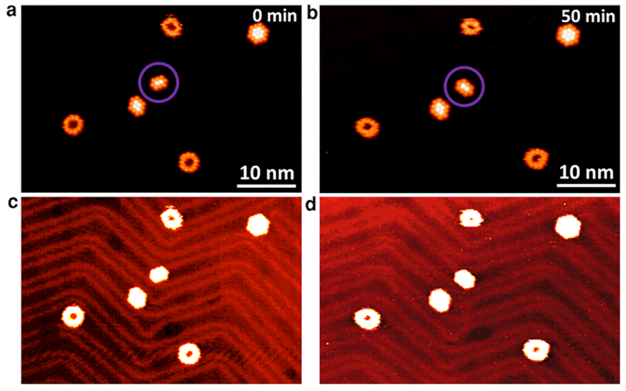

Figure 5. Flipping of a $(C_{60})_{10}$–$(Au)_{35}$ cluster at RT without the application of an STM trigger. Image in (b) is taken 50 min after the image in (a). (c,d) The same images of (a) and (b), respectively, shown with enhanced contrast so that the locations of the clusters relative to the elbows of the herringbone reconstruction become visible.

shows how a $(C_{60})_{10}$–Au_{35} cluster changes between its equivalent configurations at RT without intervention of the STM tip. Again, the cluster is not a rigid object that rotates like a rod. Instead, the "rotation" is likely facilitated by a minor disintegration of the cluster followed by reassembly. Interestingly, during the short period when the cluster is in its disintegrated state, there is sufficient attraction among the constituent atoms/molecules that prevent the loss of atoms or molecules. Temperature-induced cluster transformation without the intervention of the STM tip occurs only occasionally. The $(C_{60})_{10}$–Au_{35} cluster shown in Figure 5, for example, is observed to change once or twice within a duration of 1 h at RT. This change has a statistical nature and is probably due to thermal fluctuation within the cluster. In the absence of the STM tip, the stability of the $(C_{60})_m$–Au_n cluster is expected to be size-dependent with larger clusters being more stable. The smallest clusters, $(C_{60})_{10}$–Au_{35}, for example, are under dynamic equilibrium at RT. The molecular shell seems to be relatively stable apart from the types of changes as shown in Figure 5. The state of the Au atoms within the metal core is less clear. It is highly likely that the Au island fluctuates about its most stable form at RT. This is not surprising considering that bare Au clusters of a few tens of atoms in size readily fragment at temperatures above 230 K as observed in this study.

Theoretical simulations are performed to estimate the stability of the magic number cluster on the cascade process, as shown in Figure 6. We start with the magic number cluster

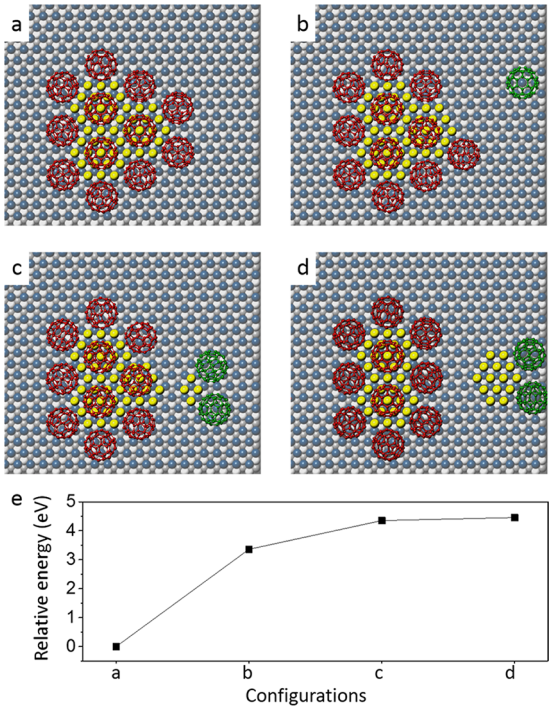

Figure 6. Calculated configurations and relative energies for disrupting a magic number $(C_{60})_{12}$–$(Au)_{49}$ cluster. (a) Top view of a perfect magic number $(C_{60})_{12}$–$(Au)_{49}$ cluster. (b) Top view of the configuration in which a C_{60} molecule is pulled away (green colored C_{60}). (c) Top view of the configuration in which two C_{60} molecules and four Au atoms are pulled away. (d) Top view of the configuration in which two C_{60} atoms and 14 Au atoms are pulled away, and the formation of a new magic number $(C_{60})_{10}$–$(Au)_{35}$ cluster. (e) The plot of relative total energies as functions of the configurations from (a)–(d). All energies are relative to the total energy of the configuration in (a).

$(C_{60})_{12}$–$(Au)_{49}$ and gradually take C_{60} molecules and Au atoms away from it. We calculate the energy corresponding to each configuration. Our calculation shows that the initial cluster is the most stable. A significant amount of energy is required to remove a C_{60} molecule to reach configuration (b). Once the "shell" of the cluster is broken, subsequent removal of more C_{60} molecules requires less energy/per molecule. The transformation from configuration (c) to (d) involves little energy change indicating this can happen spontaneously. The small fragment in (e) with two C_{60} molecules and 14 Au atoms is expected to be moving away to join other molecular islands. That would lead to some energy reduction, which is not included in the calculation. The relatively high energy required to break a stable cluster by removing a single molecule is consistent with the experimentally observed high stability of the

DOI: 10.1021/acs.nanolett.7b02802
Nano Lett. 2017, 17, 6171–6176

magic number clusters. This also gives an explanation as to why a magic number cluster, when broken by external forces, spontaneously transforms to another magic number cluster. During experiments, the energy required to break up the magic number cluster is provided by the STM tip. MD calculations are also performed to simulate the evolution of the magic number clusters (Figure S7, Supporting Information).

Cascade manipulation of $(C_{60})_m$–Au_n is a good example demonstrating the power of combining self-assembly with atom manipulation. The cluster is kept under the threshold of its thermal stability, and a single trigger from the STM tip is able to switch on a self-constructive process to reshape the cluster. Without the trigger from the STM tip, the cluster is not able to downsize itself under thermal activation. In fact, if thermal activation is provided alone, the clusters simply fall apart. The trigger provides the pathway to perturb the cluster without giving the cluster too much energy to go over the barrier for decomposition. Thermal effects always play an important role in STM-induced processes.[31,32] We have demonstrated here that thermal energy can be selectively channelled into a specific reaction process for nanoprocessing.

The trigger we apply to initiate cascade manipulation is easily controlled, and it leads to a high success rate. Nevertheless, the mechanism of extracting the very first C_{60} molecule from the hybrid cluster by the STM tip is worthy of some discussion. There is a wealth of information on the manipulation of C_{60} molecules using the STM tip.[33−35] Thermal decomposition can take place if the heating power due to the tip−sample current exceeds a certain threshold.[33,34] Thermal decomposition is unlikely to occur in our experiments where the power dissipation is low, and moreover, we were able to extract molecules with zero sample bias, hence ruling out the electric field as the major contribution. Our observation indicates that a simple repulsive interaction is responsible for the displacement of the C_{60} molecule. When the tip moves toward the cluster, it forces its way in by displacing molecules sideways and occupies the space vacated by the molecule. When the tip withdraws, the displaced molecule may return to the broken cluster. If the molecule has already moved a long distance away from the cluster before the withdrawal of the tip, it will become permanently separated from the cluster. If the trigger is applied to a molecule sitting on top of the Au island, the molecule may get pushed over the step edge of the island. Since the step edge is already fully decorated by C_{60} molecules, this will result in one molecule being squeezed out of the cluster. Such a lone molecule attached weakly to the outer perimeter of the molecular shell of the cluster can be evaporated off easily around RT.[21]

With the rapid development in high-resolution atomic force microscopy (AFM), progress has been made recently in atom manipulation with the AFM.[15,35] The advantage of the AFM is that manipulation can be conducted readily on insulating substrates. The manipulation of the $(C_{60})_m$–Au_n clusters described herein relies on the contact force between the STM tip and the molecules, so the technique can be extended to insulating surfaces with the AFM. The combination of a localized triggering event with thermal activated self-assembly has great potential as a practical technique for precision engineering at the nanometer scale.

In conclusion, cascade manipulation of magic number $(C_{60})_m$–Au_n clusters triggered by the STM tip is an efficient and accurate method for down-sizing the clusters. Instead of operating on an atom-by-atom or molecule-by-molecule basis, the STM tip is required to produce the initial trigger that disrupts the cluster. Then, the cluster takes over the reorganizational duties and evolves into a new cluster of well-defined composition and shape. In contrast to atom-by-atom assembly, which generally requires a low temperature in order to suppress thermal agitation, cascade manipulation takes full advantage of thermal energy by converting it into useful work at the nanoscale.

Experimental Methods. The substrate is a (111) oriented thin film of Au deposited onto highly oriented pyrolytic graphite (HOPG) by thermal evaporation of Au in a BOC Edward 306 evaporator. During deposition, the HOPG sample is kept at 493 K. The thickness of the Au film is ∼300 nm, measured using a quartz crystal microbalance. The Au film is transferred into an ultrahigh vacuum (UHV) chamber where the STM is located. Once inside the UHV chamber, the sample is treated by many cycles of Ar^+ ion bombardment and thermal annealing to 1000 K to provide large flat atomic terraces for in situ growth of $(C_{60})_m$–Au_n clusters. An Omicron variable temperature STM (VT-STM) with electrochemically polished W tip is used for imaging and manipulation of $(C_{60})_m$–Au_n clusters.

To obtain hybrid $(C_{60})_m$–Au_n clusters at RT, ∼0.04 monolayer (ML) of C_{60} molecules is deposited onto the Au(111) sample, which is kept at 110 K. This is followed by the deposition of ∼0.04 ML of Au atoms. Both the C_{60} molecules and the Au atoms move to the elbow sites on the herringbone reconstructed Au(111) surface. Upon annealing to RT, self-assembled $(C_{60})_m$–Au_n clusters are found to form at the elbow sites. The order of deposition can be reversed, with Au deposited before C_{60} without affecting the final outcome.

Simulation Methods. The model is built with a 20 × 20 supercell of Au(111) surface containing three atomic layers, with adsorbing Au island and C_{60} molecules on one side of the slab. The atoms in Au clusters are all adsorbed at the face-centered cubic (fcc) sites on the Au(111) surface. The size of the supercell is about 57.7 Å × 50.0 Å × 40 Å. The molecular dynamics (MD) simulations are performed in a NVT ensemble based on Nosé−Hoover thermostat at various temperatures in different time scales. For the MD simulations, the COMPASS force field is employed to investigate the interactions between C_{60} molecules and Au islands. The time step of 2 fs is used in all simulations. In the relaxation, the Au slab is frozen, while all C_{60} molecules and Au atoms in clusters are fully relaxed.

■ ASSOCIATED CONTENT

Supporting Information

The Supporting Information is available free of charge on the ACS Publications website at DOI: 10.1021/acs.nanolett.7b02802.

Derivation of optimal manipulation parameters and additional information on MD simulation (PDF)

■ AUTHOR INFORMATION

Corresponding Authors

*E-mail: q.guo@bham.ac.uk.
*E-mail: sxdu@iphy.ac.cn.

ORCID

Shixuan Du: 0000-0001-9323-1307
Quanmin Guo: 0000-0002-3417-8726

DOI: 10.1021/acs.nanolett.7b02802
Nano Lett. 2017, 17, 6171−6176

Author Contributions

D.K. performed all the experiments. D.B. performed the MD simulations. These authors made equal contributions to the manuscript. All authors contributed to data analysis and writing of the manuscript.

Notes

The authors declare no competing financial interest.

REFERENCES

(1) Busche, C.; Vila-Nadal, L.; Yan, J.; Miras, H. N.; Long, D.-L.; Georgiev, V. P.; Asenov, A.; Pedersen, R. H.; Gadegaard, N.; Mirza, M. M.; Paul, D. J.; Poblet, J. M.; Cronin, L. *Nature* **2014**, *515* (7528), 545−549.

(2) Fan, J. A.; Wu, C.; Bao, K.; Bao, J.; Bardhan, R.; Halas, N. J.; Manoharan, V. N.; Nordlander, P.; Shvets, G.; Capasso, F. *Science* **2010**, *328* (5982), 1135−1138.

(3) Liu, P.; Zhao, Y.; Qin, R.; Mo, S.; Chen, G.; Gu, L.; Chevrier, D. M.; Zhang, P.; Guo, Q.; Zang, D.; Wu, B.; Fu, G.; Zheng, N. *Science* **2016**, *352* (6287), 797−800.

(4) Emmrich, M.; Huber, F.; Pielmeier, F.; Welker, J.; Hofmann, T.; Schneiderbauer, M.; Meuer, D.; Polesya, S.; Mankovsky, S.; Ködderitzsch, D.; Ebert, H.; Giessibl, F. J. *Science* **2015**, *348* (6232), 308−311.

(5) Hernandez-Fernandez, P.; Masini, F.; McCarthy, D. N.; Strebel, C. E.; Friebel, D.; Deiana, D.; Malacrida, P.; Nierhoff, A.; Bodin, A.; Wise, A. M.; Nielsen, J. H.; Hansen, T. W.; Nilsson, A.; Stephens, I. E. L.; Chorkendorff, I. *Nat. Chem.* **2014**, *6* (8), 732−738.

(6) Desireddy, A.; Conn, B. E.; Guo, J.; Yoon, B.; Barnett, R. N.; Monahan, B. M.; Kirschbaum, K.; Griffith, W. P.; Whetten, R. L.; Landman, U.; Bigioni, T. P. *Nature* **2013**, *501* (7467), 399−402.

(7) Eigler, D. M. *Nature* **1990**, *344*, 524.

(8) Braun, K. F.; Rieder, K. H. *Phys. Rev. Lett.* **2002**, *88* (9), 096801.

(9) Hla, S. W.; Braun, K. F.; Rieder, K. H. *Phys. Rev. B: Condens. Matter Mater. Phys.* **2003**, *67* (20), 201402.

(10) Manoharan, H. C.; Lutz, C. P.; Eigler, D. M. *Nature* **2000**, *403* (6769), 512−515.

(11) Hirjibehedin, C. F.; Lutz, C. P.; Heinrich, A. J. *Science* **2006**, *312* (5776), 1021−1024.

(12) Heinrich, A. J.; Lutz, C. P.; Gupta, J. A.; Eigler, D. M. *Science* **2002**, *298* (5597), 1381−1387.

(13) Sloan, P. A.; Palmer, R. E. *Nature* **2005**, *434* (7031), 367−371.

(14) Kumagai, T.; Hanke, F.; Gawinkowski, S.; Sharp, J.; Kotsis, K.; Waluk, J.; Persson, M.; Grill, L. *Nat. Chem.* **2014**, *6* (1), 41−46.

(15) Inami, E.; Hamada, I.; Ueda, K.; Abe, M.; Morita, S.; Sugimoto, Y. *Nat. Commun.* **2015**, *6*, 6231.

(16) Kong, H.; Wang, L.; Sun, Q.; Zhang, C.; Tan, Q.; Xu, W. *Angew. Chem.* **2015**, *127* (22), 6626−6630.

(17) Lim, T.; Polanyi, J. C.; Guo, H.; Ji, W. *Nat. Chem.* **2011**, *3* (1), 85−89.

(18) Lock, D.; Rusimova, K. R.; Pan, T. L.; Palmer, R. E.; Sloan, P. A. *Nat. Commun.* **2015**, *6*, 8365.

(19) Sloan, P. A.; Sakulsermsuk, S.; Palmer, R. E. *Phys. Rev. Lett.* **2010**, *105* (4), 048301.

(20) Rusimova, K. R.; Bannister, N.; Harrison, P.; Lock, D.; Crampin, S.; Palmer, R. E.; Sloan, P. A. *Nat. Commun.* **2016**, *7*, 12839.

(21) Xie, Y.-C.; Tang, L.; Guo, Q. *Phys. Rev. Lett.* **2013**, *111* (18), 186101.

(22) Tang, L.; Zhang, X.; Guo, Q.; Wu, Y.-N.; Wang, L.-L.; Cheng, H.-P. *Phys. Rev. B: Condens. Matter Mater. Phys.* **2010**, *82* (12), 125414.

(23) Zhang, X.; Tang, L.; Guo, Q. *J. Phys. Chem. C* **2010**, *114* (14), 6433−6439.

(24) Altman, E. I.; Colton, R. J. *Surf. Sci.* **1992**, *279* (1), 49−67.

(25) Berndt, R.; Kroger, J.; Neel, N.; Schull, G. *Phys. Chem. Chem. Phys.* **2010**, *12* (5), 1022−1032.

(26) Écija, D.; Otero, R.; Sánchez, L.; Gallego, J. M.; Wang, Y.; Alcamí, M.; Martín, F.; Martín, N.; Miranda, R. *Angew. Chem., Int. Ed.* **2007**, *46* (41), 7874−7877.

(27) Sánchez, L.; Otero, R.; Gallego, J. M.; Miranda, R.; Martín, N. *Chem. Rev.* **2009**, *109* (5), 2081−2091.

(28) Schull, G.; Frederiksen, T.; Arnau, A.; Sanchez-Portal, D.; Berndt, R. *Nat. Nanotechnol.* **2011**, *6* (1), 23−27.

(29) Schull, G.; Frederiksen, T.; Brandbyge, M.; Berndt, R. *Phys. Rev. Lett.* **2009**, *103* (20), 206803.

(30) Hauptmann, N.; Mohn, F.; Gross, L.; Meyer, G.; Frederiksen, T.; Berndt, R. *New J. Phys.* **2012**, *14* (7), 073032.

(31) Sakulsermsuk, S.; Sloan, P. A.; Palmer, R. E. *ACS Nano* **2010**, *4* (12), 7344−7348.

(32) Pan, T. L.; Sloan, P. A.; Palmer, R. E. *J. Phys. Chem. Lett.* **2014**, *5* (20), 3551−3554.

(33) Schulze, G.; Franke, K. J.; Gagliardi, A.; Romano, G.; Lin, C. S.; Rosa, A. L.; Niehaus, T. A.; Frauenheim, T.; Di Carlo, A.; Pecchia, A.; Pascual, J. I. *Phys. Rev. Lett.* **2008**, *100* (13), 136801.

(34) Schulze, G.; Franke, K. J.; Pascual, J. I. *New J. Phys.* **2008**, *10* (6), 065005.

(35) Kawai, S.; Foster, A. S.; Canova, F. F.; Onodera, H.; Kitamura, S.-I.; Meyer, E. *Nat. Commun.* **2014**, *5*, 1−7.

DOI: 10.1021/acs.nanolett.7b02802
Nano Lett. 2017, 17, 6171−6176